DESIGN AND TESTING OF CO-CURED BONDED CFRP-STEEL HYBRIDS WITH NANOSTRUCTURED INTERFACES FOR INTERLAMINAR FRACTURE TOUGHNESS

Jan Striewe[1], Richard Grothe[2], Jannik Kowatz[3], Thomas Tröster[4], Guido Grundmeier[5], Gerson Meschut[6]

[1]Automotive Lightweight Design, Paderborn University, Pohlweg 47-49, 33098 Paderborn, Germany
Email: jan.striewe@uni-paderborn.de, Web Page: http://www.leichtbau-im-automobil.de
[2]Techn. Macrom. Chemistry, Paderborn University, Warburger Str. 100, 33098 Paderborn, Germany
Email: richard.grothe@uni-paderborn.de, Web Page: http://chemie.uni-paderborn.de
[3]Material and Joining Technology, Paderborn University, Pohlweg 47-49, 33098 Paderborn, Germany
Email: jannik.kowatz@lwf.uni-paderborn.de, Web Page: https://lwf.uni-paderborn.de
[4]Automotive Lightweight Design, Paderborn University, Pohlweg 47-49, 33098 Paderborn, Germany
Email: thomas.tröster@uni-paderborn.de, Web Page: http://www.leichtbau-im-automobil.de
[5]Techn. Macrom. Chemistry, Paderborn University, Warburger Str. 100, 33098 Paderborn, Germany
Email: g.grundmeier@tc.uni-paderborn.de, Web Page: http://chemie.uni-paderborn.de
[6]Material and Joining Technology, Paderborn University, Pohlweg 47-49, 33098 Paderborn, Germany
Email: meschut@lwf.uni-paderborn.de, Web Page: https://lwf.uni-paderborn.de

Keywords: CFRP-steel hybrid, surface modification, nanorods, Double Cantilever Beam, End-Notched Flexure, energy release rate

Abstract

The present work investigates co-cured bonded hybrid systems consisting of a high-strength steel with innovative surface modifications and a carbon fibre-reinforced (thermoset) plastic (CFRP) regarding interfacial fracture toughness. As main surface modification, zinc oxide (ZnO) nanorods are formed on a hot-dip galvanized steel substrate by means of hydrothermal deposition from an aqueous solution. Based on this crystalline surface morphology, additional adhesion promoter systems Aminopropyl-triethoxysilane (APTES) and Aminopropyl Phosphonic Acid (APPA) are considered. Due to diverse mechanical and thermal characteristics of CFRP and steel, a methodical design of asymmetric Double Cantilever Beam (DCB) specimens is stated. Amongst others, this includes the decoupling of Mode I and Mode II behaviour by approximation. Interlaminar fracture toughnesses are determined using image recording or digital image correlation (DIC) methods as well as visual onset of delamination. Concluding, the investigated surface modifications based on nanorods significantly improve the adhesion to the thermosetting resin compared to grit blasting and / or alkaline cleaning of the metal substrate.

1. Introduction

Today, mass savings through lightweight design are of great importance in many industrial sectors. In case of vehicles with internal combustion engines, this approach contributes to an increase in efficiency and thus to a reduction in carbon dioxide (CO_2) emissions [1]. Materials with advantageous weight-specific material properties, such as fibre-reinforced plastics (FRP), are notably suitable for lightweight design and therefore increasingly establishing themselves in automotive body structures [2, 3]. Against this background, the local and load-adapted reinforcement of non-uniformly stressed metal structures is

a significant field of application for carbon fibre-reinforced plastics. Such tailored hybrid structures combine a considerable potential for weight savings with moderate additional costs [4].

Adhesive bonding offers several advantages compared to mechanical fastening techniques. This can be a lower weight, reduced manufacturing costs or a more uniform stress distribution [5]. For this reason, the manufacturing of hybrid systems by co-cured bonding, which combines the curing of the thermoset resin with the bonding to a solid substrate into one process step, is a promising approach. A prerequisite for the technical use of co-cured hybrid systems is a mechanically strong bond between the constituent materials. To achieve a sufficient strength of adhesive bonds, literature depicts a variety of conditioning methods of metal substrates e.g. by mechanical, physical or chemical treatment. In this context, a rise in adhesion strength results from a higher surface tension, an increase in surface roughness on a macro and / or microscopic level or the generation of a clean and stable cohesion layer [6].

The aim of the present work is the analysis and evaluation of the effectiveness of an innovative chemical surface treatment on a zinc coated steel substrate regarding interfacial adhesion to CFRP. Chemical pre-treatments are based on crystal growth of zinc oxide nanorods and two complementary adhesion-promoting systems. The experimental investigations based on ASTM D5528 and ASTM D7905 are preceded by a methodical design of test specimen comparable to Yüksel et al. [7].

2. Materials and surface modifications

As composite material, carbon fibres with a dry-fibre area weight of 300 g/m² and a fast curing epoxy resin were used. In cured stage, the layer thickness corresponds to 0.3 mm. Furthermore, a cold-rolled dual-phase steel with a tensile strength of 800 MPa was utilised with a thickness of 2.0 mm. On delivery condition, the hot-dip galvanized steel sheets had a zinc coating thickness of approx. 7 µm (Z100).

For experimental tests, the surface of the metal substrates was chemically modified by the growth of zinc oxide nanorods [Fig. 1]. To synthesize this nanoscale coating on the steel substrate, an equimolar solution of $Zn(NO_3)_2 \cdot 6H_2O$ and Hexamethylenetetramine $C_6H_{12}N_4$ was used [8, 9]. The concentration was 0.1 M each. In a first step, the samples were cleaned in a three stage cleaning process with tetra hydro furan (THF), iso-propanol (IPA) and ethanol (EtOH) for 10 min each in an ultrasonic bath at room temperature and dried with nitrogen. Afterwards, the substrates were cleaned in an alkaline solution of Ridosol (3 g/l) and Ridoline (30 g/l) for 30 sec at 55 °C, rinsed with ultraclean water and, again, dried in a nitrogen stream. For the coating of the substrates, the solutions were separately heated to 95 °C and then merged in a lockable and pressure-resistant container. The container was placed in a temperate water bath for 30 min. Following, the samples were cleaned with ultraclean water and dried in nitrogen.

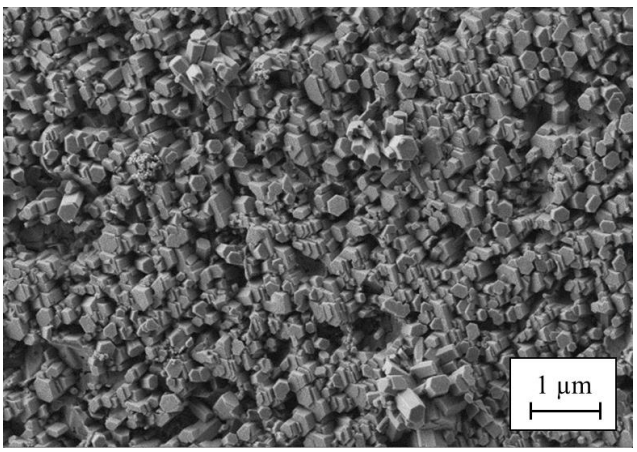

Figure 1. SEM micrograph of a zinc oxide nanostructured steel surface.

In addition to the zinc oxide nanocoating, two adhesion promoter systems were optionally applied. These are Aminopropyltriethoxysilane (APTES) and Aminopropyl Phosphonic Acid (APPA) which were used with a concentration of 1 V-% in case of the amino silane and 1 mM for the amino phosphonic acid. The silane was solved in ethanol with additionally 1 V-% of water to activate the triethoxysilane group, hydrolysing it to a trisilanol- and three single ethanol groups. The amino phosphonic acid was solved in water only. While the APPA solution has a neutral pH between 6 and 7, the APTES solution has an alkaline pH value at 12. According to Wapner et al. [10], this significantly affects the chemical reaction properties of ZnO nanorods. The samples were full immersed in those solutions for 1 h at room temperature. After this dip coating process the sample surfaces were rinsed with ethanol in case of the APTES and with water in case of the APPA. After drying of the sample surfaces in a nitrogen stream they were tempered in an oven at 60 °C for 1 h. As reference systems for the specified chemical surface treatments, an abrasive mechanical treatment of the initial zinc coating by grit blasting with regular aluminium oxide (particle size: 210-297 µm) as well as the cleaning of the metal substrate by an alkaline solvent were considered in experimental tests.

3. Specimen design

The specimen design is based on specifications in ASTM D5528 and ASTM D7905. In accordance to these standards, the specimen length (175 mm), width (25 mm) and maximum thickness (4.7 mm) were chosen. Due to the 2.0 mm thick steel substrate, the maximum composite thickness amounts to 2.7 mm or nine layers of CFRP in cured stage.

A uniform deflection of beam arms with dissimilar materials and thus the decoupling of Mode I and Mode II behaviour was considered following Eq. 1 with bending moduli E_i and component thicknesses h_i. As stated by Ouyang et al. [11], this equation implies that Mode I loading exclusively depends on the normal stress of the boundary layer through crack opening while Mode II behaviour solely results from shear stresses due to relative displacements at the interface.

$$E_{CFRP} \cdot {h_{CFRP}}^2 = E_{steel} \cdot {h_{steel}}^2 \quad (1)$$

Since the material properties of multi-layered composites depend on the number, the orientation and the stacking sequence of the layers, various combinations of the global flexural modulus and composite thickness comply with the defined geometrical requirements. For this reason, in-plane fibre orientations were limited to 0° (parallel to the longitudinal specimen axis) and 90° (orthogonal to the specimen longitudinal axis). Furthermore, a mid-symmetric stacking sequence and 0°-layers on the top and the bottom line of the CFRP laminate were set as required. Based on these specifications, the theoretic bending moduli for permissible composite stacking sequences were calculated using classical laminate theory (CLT) for laminates with seven to ten layers. Afterwards, these values were multiplied by the square of the corresponding laminate thickness and plotted against h_{CFRP} (Fig. 2).

Further analytical considerations were based on thermally induced residual stresses of the asymmetric hybrid compound due to different and directionally dependent thermal expansion coefficients of the materials contained. This led to a composite stacking sequence according to ($0_3/90_3/0_3$), as it exhibits minimal thermal induced deflections.

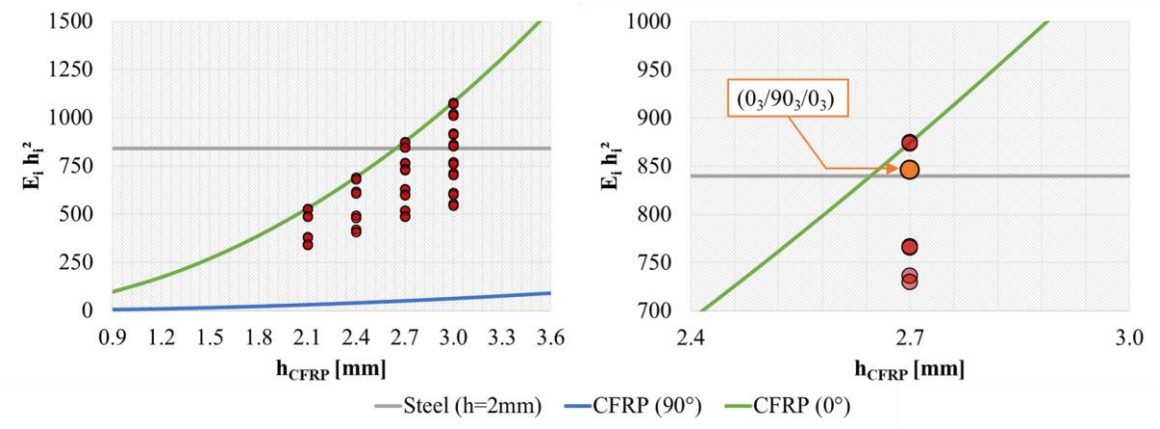

Figure 2. Methodical laminate design.

4. Specimen manufacturing and preparation

Test specimens were produced by means of co-cured bonding. Therefore, preimpregnated fibre layers were stacked on the modified metal substrates. At the interface, a precrack was built in using an ETFE-foil with a thickness of 12.5 µm. The composite layup was calendered and then subjected to heat and pressure in a mould cavity. Simultaneously to the curing of the resin, the bond between the polymer and the metal substrate was established. A consolidation pressure of 0.3 MPa and a mould temperature of 120 °C for 10 min were used for the curing cycle. Residual curing took place in the context of a cathodic dip painting with downstream drying procedure at elevated temperatures. Furthermore, metallic load blocks were applied using a cold-curing two-component adhesive in the case of Double Cantilever Beam specimens. For the analysis of crack propagation, samples were provided with a line scale (DCB) or a high contrast stochastic pattern (ENF) on one of the lateral sample sides.

5. Experimental setup and results

To investigate the interlaminar energy release rate under crack opening load (Mode I), the test specimens were loaded via the load blocks at a constant crosshead speed of 2.0 mm / min. In contrast, the energy release rate under shear stress of the boundary layer (Mode II) was investigated by a three-point bending procedure with a bearing distance of 100 mm up to initial, mostly unstable crack propagation. The loading through the punch was applied at a constant rate of 0.5 mm / min. In both cases, the resulting forces, the traverse movement and the course of the crack propagation was recorded and synchronized by accompanying image recording and digital image correlation methods, respectively.

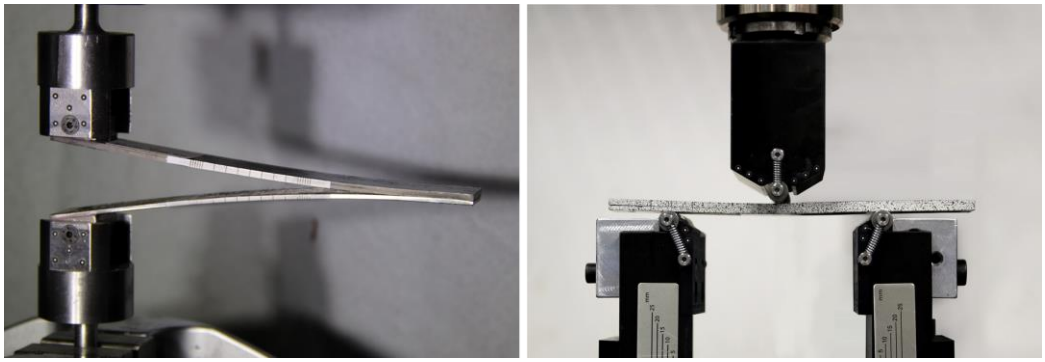

Figure 3. Double Cantilever Beam and End-Notched Flexure tests.

According to ASTM D5528 or ASTM D7905, energy release rates were calculated using the Modified Compliance Calibration Method (MCCM) or the Compliance Calibration Method (CCM). The assessment of interface fracture was based on visual delamination onset. For evaluation of the Double Cantilever Beam tests, correction factors for large displacements and the stiffening of the specimens by the load blocks were taken into account.

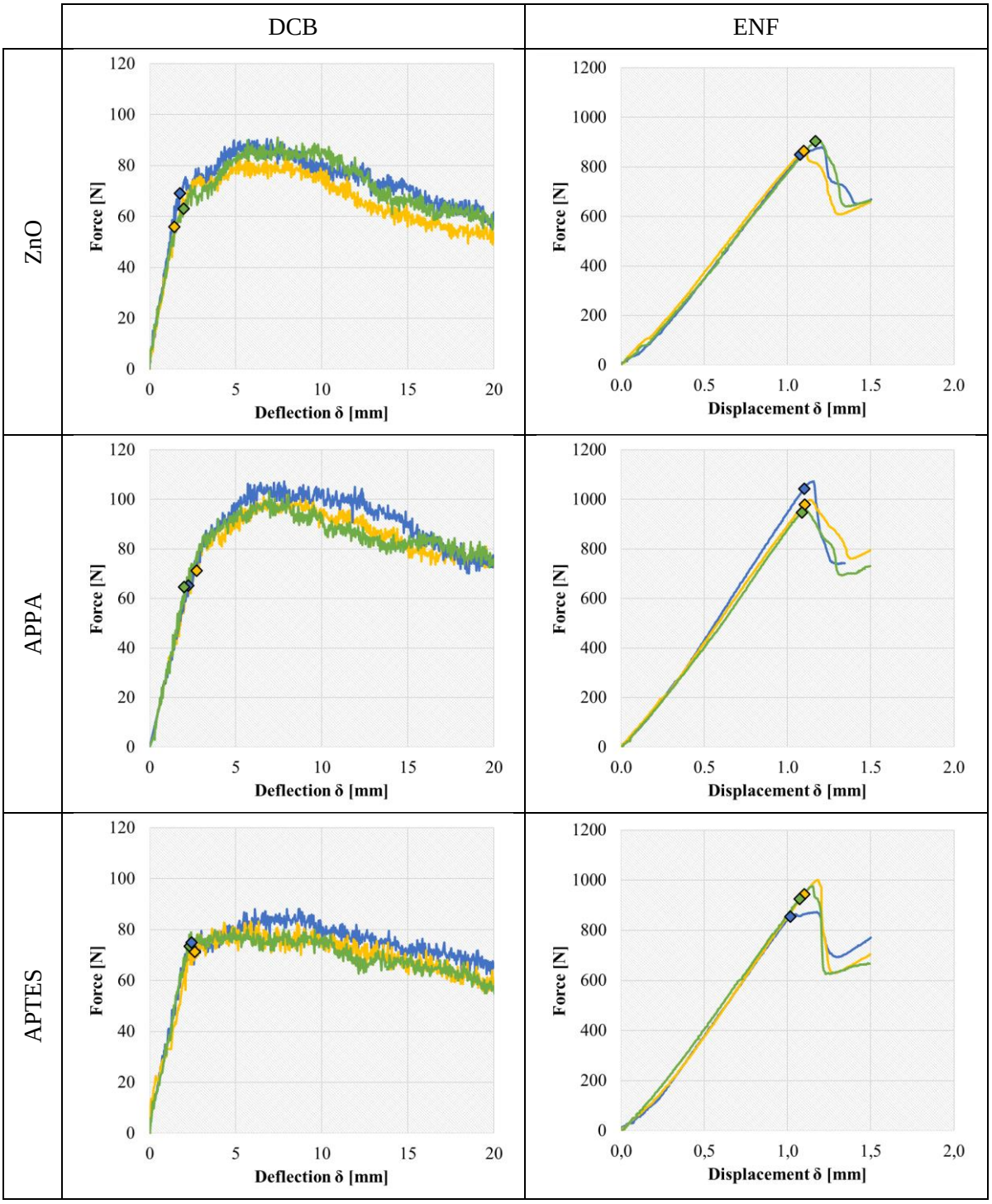

Figure 4. F-δ diagrams of DCB and ENF tests with visual delamination onset.

In the presented DCB studies, the solitaire ZnO coating achieved a mean maximum force of 89 N. Furthermore, the applied adhesion promoter APPA significantly increased this average force to about 104 N. The second adhesion promoter system APTES, however, resulted in a comparatively low maximum force of 84 N. Nevertheless, the visually determined onset of delamination led to the highest G_{IC} of 166 J / m² in comparison (Figure 5, Table 1). The exclusively alkaline-cleaned reference surface caused the interfacial connection to be dissolved during the electrophoretic dip-coating process. Amongst others, this could be a result of elevated temperatures above the glass transition T_g of the polymer and comparatively poor bonding properties (e.g. based on undercuts). Pre-treatment by sandblasting resulted in a bond more resistant to cathodic dip-coating and drying, although the average G_{IC} (79 J / m²) was significantly lower than that of the zinc oxide nanocoat.

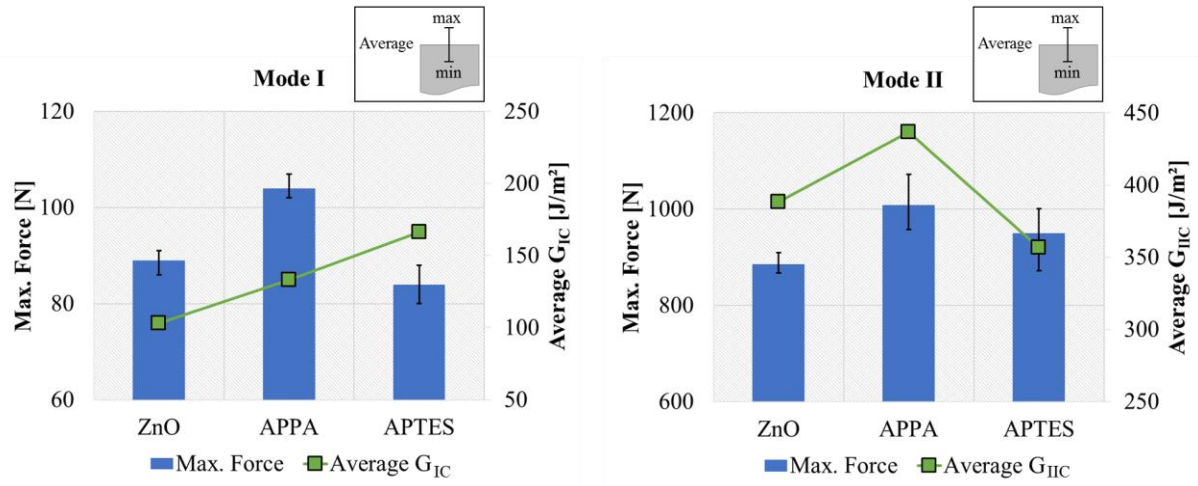

Figure 5. Maximum forces and average G_C-values of DCB and ENF tests.

As part of the ENF experiments, the highest forces were achieved by the zinc oxide coating with additional adhesion promoter APPA, analogous to the results of the DCB tests. These average around 1009 N, which is about 14 % higher than the exclusively zinc oxide coated samples. The adhesion promoter APTES achieved an increase of 7 %. In contrast to Mode I loading, the highest maximum force of APPA correlates with the highest G_{IIC} value of 437 J / m². In addition, the zinc oxide nanorods (388 J / m²) resulted in a higher energy release rate under Mode II loading than the additional APTES coating (357 J / m²). The grit blasted reference modification achieved an energy release rate of 149 J / m². Overall, it should be noted that the alignment of the asymmetric hybrid compound (here: stamp-side arrangement of the CFRP) can have a significant influence on the Mode II behaviour, e.g. as a consequence of thermally induced residual stresses. For this reason, the validity and transferability of determined values is limited.

Table 1. Calculated G_{IC} and G_{IIC} values based on visual delamination onset.

	ZnO	APPA	APTES
$G_{IC, VIS}$ [J / m²]	103	133	166
$G_{IIC, VIS}$ [J / m²]	388	437	357

6. Conclusions

In the present work, the adhesion properties of co-cured bonded surface-modified steel and carbon fibre-reinforced plastic hybrid systems were examined for interfacial fracture toughness. For this purpose, a hydrothermal deposition process of ZnO nanorods from an aqueous solution on a galvanized steel substrate was demonstrated. The experimental investigation and evaluation of the adhesion properties between steel substrate and CFRP under Mode I and Mode II loading were performed with Double Cantilever Beam and End-Notched-Flexure tests. For this purpose, the methodical design of asymmetric test specimens consisting of dissimilar materials was presented. Interlaminar fracture toughnesses were determined by visual onset of delamination. By the zinc oxide nanostructures, the bond strength at the interface was qualitatively improved under crack opening and sliding as compared to an alkaline cleaned or grit blasted substrate surface. However, thermally induced deformations and residual stresses of asymmetric hybrid specimens remain a central challenge for determining reliable energy release rates. Therefore, alternative test methods may be required for an accurate assessment of Mode I and Mode II behaviour.

Acknowledgments

The CORNET promotion plan (Nr. 19246) of the Research Community for Quality (FQS), August-Schanz-Straße 21A, 60433 Frankfurt/Main has been funded by the AiF within the programme for sponsorship by Industrial Joint Research (IGF) of the German Federal Ministry of Economic Affairs and Energy based on an enactment of the German Parliament.

References

[1] J. C. Kelly, J. L. Sullivan, A. Burnham, A. Elgowainy. Impacts of Vehicle Weight Reduction via Material Substitution on Life-Cycle Greenhouse Gas Emissions. Environ Sci Technol, Vol. 49 (20), 12535–12542, 2015.

[2] J. Starke. Carbon composites in automotive structural applications. Proceedings of the EuCIA: Composites and Sustainability, Brussels, Belgium, March 19 2016.

[3] R. Stewart. Automotive composites offer lighter solutions. Reinforced Plastics, Vol. 54, 22-28, 2010.

[4] J.G. Broughton, A. Beevers, A.R. Hutchinson. Carbon-fibre-reinforced plastic (CFRP) strengthening of aluminium extrusions. International Journal of Adhesion and Adhesives, Vol. 17, No. 3, 269-278, 1997.

[5] M. Heshmati, R. Haghani, M. Al-Emrani. Environmental durability of adhesively bonded FRP/steel joints in civil engineering applications: State of the art. Composites Part B: Engineering, Vol. 81, 259-275, 2015.

[6] A. Baldan. Adhesively-bonded joints and repairs in metallic alloys, polymers and composite materials: Adhesives, adhesion theories and surface pretreatment. Journal of Materials Science, Vol. 39, 1-49, 2004.

[7] F. Yüksel, R. Hinterhölzl, K. Drechsler. Direct adhesion of CFR-thermoplast on steel – testing and simulation oft he lap shear fracture. Proceedings of the 17th European Conference on Composite Materials, Munich, Germany, June 26-30, 2016.

[8] X. Ma, M. Gao, J. Zheng, H. Xu, G. Li, Conversion of large-scale oriented ZnO rod array into nanotube array under hydrothermal etching condition via one-step synthesis approach. Physica E: Low-dimensional Systems and Nanostructures, Vol. 42, 2237–2241, 2010.

[9] O. Ozcan, K. Pohl, B. Ozkaya, G. Grundmeier. Molecular Studies of Adhesion and De-Adhesion on ZnO Nanorod Film-Covered Metals. The Journal of Adhesion, Vol. 89, 128–139, 2013.

[10] K. Wapner, M. Stratmann, G. Grundmeier. Structure and stability of adhesion promoting aminopropyl phosphonate layers at polymer/aluminium oxide interfaces International Journal of Adhesion and Adhesives. Vol 28, 59–70, 2008.

[11] Z. Ouyang, G. Ji, G. Li. On Approximately Realizing and Characterizing Pure Mode I Interface Fracture Between Bonded Dissimilar Materials. Journal of Applied Mechanics, Vol. 78, 2011.